Ilam University of Medical Sciences

Plant Biotechnology Persa

Online ISSN: 2676-7414

Homepage: https://pbp.medilam.ac.ir

Combined Antiproliferative Effects of Naringin and Capecitabine in MCF-7 and SK-BR-3 Breast Cancer Cells

Sanli Soltannezhad[1], **Laya Takbiri Osgoei**[1]✉, **Fatemeh Javani Jouni**[2, 3]

[1] Department of Biochemistry, NT.C., Islamic Azad University, Tehran, Iran
[2] Laser Application in Medical Sciences Research Center, Shahid Beheshti University of Medical Sciences, Tehran, Iran
[3] Department of Biochemistry and Biophysics, TeMS.C., Islamic Azad University, Tehran, Iran

Article Info

Article type:
Original Article

Article History:
Received: 29 July 2026
Revised: 03 Sep 2026
Accepted: 05 Sep 2026
Published Online:

✉ ***Correspondence to:***
Laya Takbiri Osgoei

Email:
l.takbiri@iau.ac.ir

A B S T R A C T

Objective: Breast cancer is one of the most common malignancies among women, and natural compounds are increasingly investigated as adjuncts to conventional chemotherapy. This study evaluated the combined antiproliferative and pro-apoptotic effects of naringin and capecitabine in MCF-7 and SK-BR-3 breast cancer cell lines.

Methods: Cell viability was assessed by MTT assay after treatment with each compound alone and in paired combinations, and drug interactions were explored using the Combination Index (CI). Bax, Bcl-2, and Caspase-3 expression was measured by quantitative real-time PCR.

Results: Curve-extrapolated IC50 estimates of naringin were 58 and 56.65 µg/mL in MCF-7 and SK-BR-3 cells, respectively, while the corresponding capecitabine estimates were 619.36 and 679.51 µg/mL. Paired treatments reduced cell viability in a concentration-dependent manner. CI values were below 1 at all four tested combinations in MCF-7 cells and at three of four combinations in SK-BR-3 cells; the lowest-dose combination in SK-BR-3 yielded a CI of 1.437. Because only a limited number of paired concentrations were tested, these results were interpreted as exploratory evidence of enhanced drug interaction rather than definitive pharmacological synergy.

Conclusion: Combination treatment increased the Bax/Bcl-2 expression ratio and produced a numerically greater apoptotic response than individual treatments. Antiproliferative activity was greater in SK-BR-3 cells under the tested conditions, but this difference cannot be attributed specifically to HER2 status. Overall, naringin may enhance capecitabine activity, warranting confirmation using broader dose-response matrices and mechanistic studies.

Keywords: Naringin, Capecitabine, Breast cancer, MCF7, SK-BR-3, Apoptosis

➢ **How to cite this paper**
Soltannezhad S, Takbiri Osgoei L, Javani Jouni F. Combined antiproliferative effects of naringin and capecitabine in MCF-7 and SK-BR-3 breast cancer cells. Plant Biotechnology Persa. 2026; 8(4): Proof.

Introduction

Cancer is one of the main and most complex health concerns worldwide, which ranks second among the causes of mortality after heart disease [1]. Breast cancer, acute lymphoid leukemia cancer, stomach cancer, lung cancer, prostate cancer, colon cancer, and brain cancer are among the cancers with high mortality rates [2,3]. In 2008, 8 million deaths were recorded as a result of malignant diseases, and this number is estimated to reach 11 million by 2030 [4]. BC has been recognized as an increasing problem among women in recent years and is the most common cancer in women after non-melanoma skin cancer. Breast cancer has five molecular subtypes, including luminal A, luminal B, ERBB2, basal-like, and normal-like [5]. Estrogen receptor (ER)-positive and HER2-negative (ER+/HER2−) BC accounts for approximately 70% of all breast cancer cases. HER2 expression is one of the most important molecular markers for breast cancer, and 15-25% of women with breast cancer have HER2 [6]. Tumor characteristics determine which type of treatment patients with breast cancer will benefit from. For example, patients with human

DOI:
Publisher: Ilam University of Medical Sciences

epidermal growth factor receptor 2-positive ($HER2^+$) cancer benefit from treatment using HER2-directed therapies [7].

Capecitabine is an oral anti-fluoropyrimidine deoxynucleoside carbamate drug that is converted to 5-fluorouracil by thymidine phosphorylase in patients and then accumulates in cancer tissue [8,9]. Capecitabine is effective in the adjuvant setting for patients with $HER2^-$ and $HER2^+$ breast cancer. It has also been approved for adjuvant treatment of metastatic breast cancer after the use of anthracyclines and taxanes [10,11]. Considering the ability of adavosertib to increase the efficiency of DNA-damaging agents, capecitabine is a suitable combination partner for adavosertib. Capecitabine has been used in combination with other agents such as pyrotinib, neratinib, and lapatinib for the treatment of $HER2^+$ metastatic breast cancer. Also, the combination of capecitabine with bevacizumab has been used in the treatment of $HER2^-$ cancer, and mortality has decreased in these people [12,13].

Natural compounds have many uses, such as anti-cancer, antimicrobial, anti-inflammatory, pain-relieving properties, etc., which are widely used in finding new drugs [14,15]. Naringin, with the chemical name 5,7,4′-trihydroxyflavanone-7-O-rhamnoglucoside, is a common dietary flavanone glycoside obtained from citrus fruits. This compound was first found by De Vry in grapefruit blossoms in 1857. Naringin has been reported to have various medicinal benefits such as antioxidant, anti-apoptotic, antimicrobial, anti-inflammatory, and anti-mutagenic activities. Naringin can inhibit the biological function of the breast, thyroid, and cervical cancer cells by inhibiting the excessive activation of the PI3K/AKT/mTOR signaling pathway. Combined cancer treatment strategies with chemotherapy and natural polyphenols (naringin) may increase therapeutic potential and help reduce the side effects of anticancer treatments [16]. Therefore, we aimed to investigate the combined effect of capecitabine and naringin on $HER2^-$ and $HER2^+$ human breast cancer cells.

Materials and Methods

The antiproliferative effect of capecitabine and naringin was investigated on SK-BR-3 and MCF-7 cells, obtained from Pasteur Institute (Tehran, Iran). The DMEM medium contained 10% fetal bovine serum (FBS), 1% L-glutamine, 100 IU/mL penicillin-streptomycin. SK-BR-3 and MCF-7 cells were propagated in an incubator at 37°C with 95% humidity and 5% CO2.

Cell Culture and Mycoplasma Contamination Test

The antiproliferative effects of capecitabine and naringin were assessed on SK-BR-3 and MCF-7 cells, which were obtained from the Pasteur Institute (Tehran, Iran). The cells were cultured in DMEM medium containing 10% fetal bovine serum (FBS), 1% L-glutamine, and 100 IU/ml penicillin-streptomycin. The incubation conditions for the SK-BR-3 and MCF-7 cells were maintained at 37 °C with 95% humidity and 5% CO2. *Mycoplasma* contamination was tested using the EZdetect™ PCR kit (HiMedia Laboratories, Mumbai, India). Cells were cultivated in DMEM medium supplemented with 10% FBS, without the use of antibiotics. A 2 ml sample of supernatant from the cultured cells was collected into a microtube and centrifuged at 13,000 rpm for 30 min. The resulting pellet was resuspended in 50 µL of 1xTE buffer, vortexed, and heated at 95 °C for 10 min. The supernatant obtained after a second centrifugation was used as the PCR template. PCR was performed according to the manufacturer's instructions, using appropriate reagents and cycling conditions. Both positive and negative controls were included in the reaction. The PCR products were then visualized on a 2% agarose gel using a UV gel documentation system.

Cytotoxic evaluation of the compounds

Capecitabine and naringin were evaluated for their cytotoxic effects on MCF-7 and SK-BR-3 breast cancer cells using the MTT [3-(4,5-dimethylthiazol-2-yl)-2,5-diphenyltetrazolium bromide] assay. Logarithmically growing cells were seeded at a density of 10,000 cells/well in 96-well plates and allowed to attach for 24 h. The cells were then treated separately with different concentrations of capecitabine or naringin. Concentration ranges were used to generate dose–response curves and determine the IC50 value of each compound. Because the estimated 50% inhibitory concentrations of the individual compounds were slightly above the highest concentrations directly represented in the reported dose range, these values were obtained by nonlinear regression of the dose–response curves and are therefore reported as curve-extrapolated IC50 estimates. For the combination-treatment experiments, capecitabine was used at concentrations of 75, 150, 300, and 600 µg/mL, whereas naringin was used at concentrations of 10, 20, 30, and 40 µg/mL. Four paired combinations were therefore evaluated: 10 µg/mL naringin + 75 µg/mL capecitabine, 20 µg/mL naringin + 150 µg/mL capecitabine, 30 µg/mL naringin + 300 µg/mL capecitabine, and 40 µg/mL naringin + 600 µg/mL capecitabine. After 24 h of treatment, 20 µL of MTT solution (5 g/L) was added to

each well, and the plates were incubated for an additional 4 h. The culture medium was then removed, and 150 µL of DMSO was added to dissolve the resulting formazan crystals. Absorbance was measured at 545 nm using an ELISA plate reader (Awareness, USA). MTT assays were performed in three independent biological experiments (n = 3), with each treatment condition assessed in technical triplicate within each experiment. The mean value of the technical replicates was used as the value for each independent experiment. The IC50 values were determined from the corresponding dose–response curves using GraphPad Prism version 8. The calculated IC50 concentrations were subsequently used in the indicated downstream experiments. Cell viability for each treatment was calculated relative to the untreated control using Equation (1):

$$\text{Viability of cells (\%)} = \frac{\text{The mean absorbance of treated cells in each well}}{\text{The mean absorbance of control cells (DMSO)}} \times 100 \qquad (1)$$

Investigation of apoptosis by flow cytometry

Apoptotic cell death was evaluated by dual staining with Annexin V-FLUOS and propidium iodide (PI). For MCF-7 cells, treatments were performed for 24 h with 58 µg/mL naringin, 619.36 µg/mL capecitabine, or a combination of 30.01 µg/mL naringin and 300.03 µg/mL capecitabine. For SK-BR-3 cells, the corresponding treatments were 56.65 µg/mL naringin, 679.51 µg/mL capecitabine, or the combination of 32.06 µg/mL naringin + 361.8 µg/mL capecitabine. Untreated cells were used as controls. Following treatment, approximately 1 × 10^6 cells were collected and stained with Annexin V-FLUOS and PI according to the manufacturer's instructions. Samples were analyzed using an AQUIOS CL flow cytometer (USA). Cells were classified into four populations: viable cells, early apoptotic cells, late apoptotic cells, and necrotic cells. Flow-cytometric analyses were performed in three independent biological experiments (n = 3).

Examining the expression of Bax, Bcl-2 and Caspase-3 genes

At first, total cellular RNA was extracted using the GeneAll kit (South Korea) and was treated with DNase enzyme to ensure that there was no DNA in the product. The conditions of DNase treatment were as follows: 10 microliters of extracted RNA with 1 microliter of enzyme buffer and 2 microliters of DNase enzyme at 37°C for 5 min and then at 80°C for 5 min. The RNA sample (0.2 µg) was converted into cDNA according to the manufacturer's recommendations using Oligo (dT) 18 reverse transcriptase cDNA primers by Yekta Tajhiz Azma cDNA synthesis kit (Yekta Tehiz Azma, Tehran, Iran).

The synthesized cDNA mixture was heated at 85 °C for 5 seconds and then incubated at 42 °C for 60 min, followed by inactivation at 85 °C for 5 min. The cDNA sample was subjected to reverse transcriptase polymerase chain reaction (RT-PCR) to check the expression of *Bax*, *Bcl-2*, and *Casp3* genes by specific primers designed by Primer3 software (Table I). Finally, the data were analyzed by measuring the relative expression of $2^{-\Delta\Delta Ct}$. Gene-expression analyses were performed in three independent biological experiments (n = 3), with qPCR reactions assessed in technical replicates.

Table 1: Primer sequences used for quantitative real-time PCR analysis of Bax, Bcl-2, Caspase-3, and GAPDH

Gene	Primer sequence
Bax-F	TGCTTCAGGGTTTCATCCA -3′-5′
Bax -R	GACACTCGCTCAGCTTCTTG -3′-5′
Bcl-2-F	GATAACGGAGGCTGGGTAGG- 3′-5′
Bcl -2-R	CCAGAGGAGGAGGTAGGGAC-3′-5′
Casp3-F	GTTTGAGCCTGAGCAGAGACAT-3′-5′
Casp3-R	GGCAGCATCATCCACACATACC -3′-5′
GAPDH-F	AGGGCTGCTTTTAACTCTGG -3′-5′
GAPDH-R	CCCCACTTGATTTTGGAGGG -3′-5′

Determining lipid peroxidation index (MDA)

MDA level in the cell supernatant was measured by Nalondi™ Lipid Peroxidation Assay Kit (NID) (Navand Salamat, Iran). The MDA reaction with thiobarbituric acid reactive substances (TBARS) was the basis of the analysis. The absorbance at 532 nm was measured by a spectrophotometer and distilled water used as a blank. The results were expressed as nmol ml^{-1}. MDA measurements were performed in three independent biological experiments (n = 3).

Release of lactate dehydrogenase (LDH)

LDH level in the cell supernatant was measured by colorimetric method with LDH Assay Kit (ab102526, Abcam, Cambridge, MA, USA). The measurements were performed according to the manufacturer's instructions, and the results were expressed as U L^{-1}. LDH measurements were performed in three independent biological experiments (n = 3).

Statistical analysis

One-way ANOVA and Tukey or Tamhane test was used for statistical analysis of the quantitative variables. IC_{50} value was calculated by GraphPad Prism V8 software for each compound. Drug-interaction analysis was performed using CompuSyn software. For each treatment condition, the fraction affected (Fa) was derived from the MTT viability data, and the corresponding single-agent and combination dose–response data were entered into the software for CI calculation. The four paired combinations evaluated were 10 + 75, 20 + 150, 30 + 300, and 40 + 600 µg/mL naringin + capecitabine, respectively. Because these combinations did not constitute a constant-ratio design, the resulting CI values were interpreted as exploratory measures of drug interaction rather than definitive evidence of pharmacological synergy. According to the conventional CI interpretation, CI < 1 indicates synergistic interaction, CI = 1 an additive interaction, and CI > 1 an antagonistic interaction.

Results

Nonlinear regression of the dose–response data yielded curve-extrapolated IC50 estimates of 58 and 56.65 µg/mL for naringin in MCF-7 and SK-BR-3 cells, respectively, and 619.36 and 679.51 µg/mL for capecitabine, respectively. Because these estimates extended beyond the highest directly tested concentrations reported in the dose–response series, they should be interpreted cautiously. For the combination-treatment experiments, four paired concentrations of naringin and capecitabine were

evaluated: 10 µg/mL naringin + 75 µg/mL capecitabine, 20 µg/mL naringin + 150 µg/mL capecitabine, 30 µg/mL naringin + 300 µg/mL capecitabine, and 40 µg/mL naringin + 600 µg/mL capecitabine. In MCF-7 cells, the corresponding cell-viability percentages were 75.75 ± 4.41%, 59.85 ± 0.51%, 48.05 ± 1.44%, and 40.60 ± 1.27%, respectively. In SK-BR-3 cells, the corresponding cell-viability percentages were 82.56 ± 1.17%, 66.37 ± 0.77%, 50.53 ± 0.54%, and 41.01 ± 2.01%, respectively. These values specifically represent the paired naringin–capecitabine treatments. The dose–response profiles of naringin and capecitabine administered individually are presented separately in Figure 1A and Figure 1B, whereas the corresponding combination treatments are shown in Figure 1C. Table 2 shows the CI values for both investigated cell lines. In MCF-7 cells, the CI values were below 1 at all tested combinations. In SK-BR-3 cells, the lowest-dose combination of 10 µg/mL naringin + 75 µg/mL capecitabine yielded a CI of 1.437, indicating an antagonistic interaction according to the CI criterion. At the higher tested combinations, the CI values were below 1. These findings indicate predominantly enhanced inhibitory interactions at the tested combinations; however, given the limited number of concentration pairs evaluated, they should not be interpreted as definitive evidence of pharmacological synergy (Table 2).

Table 2: CI values calculated for the combination of naringin and capecitabine at different concentration on MCF-7 and SK-BR-3 cell lines

Naringin concentration (µg/mL)	Capecitabine concentration (µg/mL)	CI values for MCF-7 cell lines	CI values for SK-BR-3 cell lines
10	75	0.648	1.437
20	150	0.228	0.38
30	300	0.13	0.138
40	600	0.108	0.088

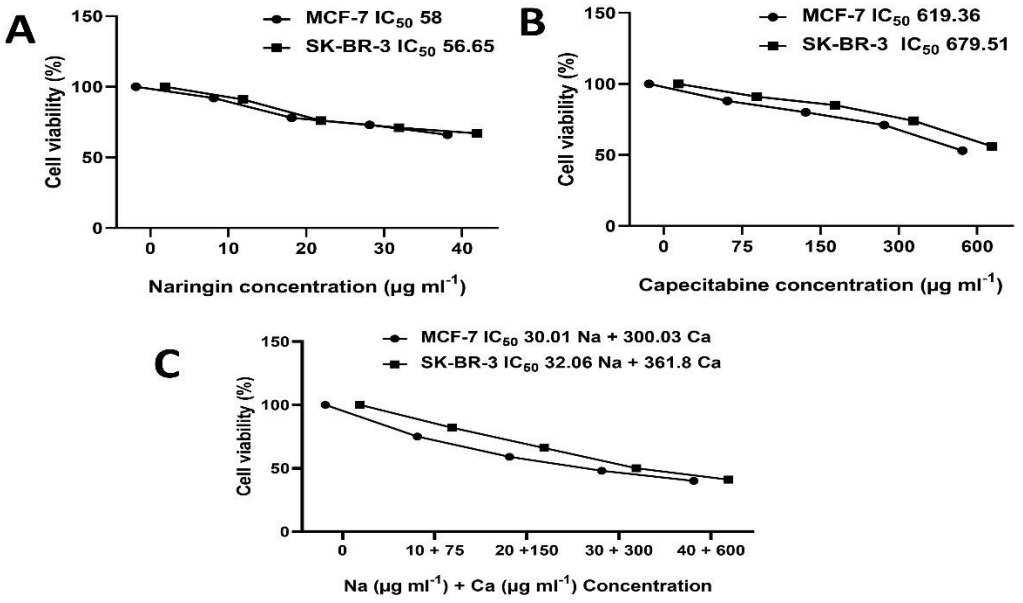

Figure 1: Cytotoxic effects of naringin alone (A), capecitabine alone (B), and their combination (C) on MCF-7 and SK-BR-3 cells. Data are presented as mean ± SD of three independent biological experiments (n = 3). Na, naringin; Ca, capecitabine

Apoptotic cell death was assessed by flow cytometry using Annexin V-FITC/PI staining in MCF-7 and SK-BR-3 cells (Figure 2). Naringin treatment resulted in apoptosis rates of 35.69% and 35.85% in MCF-7 and SK-BR-3 cells, respectively, whereas capecitabine treatment resulted in apoptosis rates of 39.39% and 37.54%, respectively. The combination treatment produced apoptosis rates of 42.09% in MCF-7 cells and 44.94% in SK-BR-3 cells. Although these values were numerically higher than those observed with the individual treatments, the increase associated with the combination did not reach statistical significance. Accordingly, these findings indicate a numerically enhanced apoptotic response following combined treatment, but they should not be interpreted as direct evidence of synergistic induction of apoptosis. Treatment with naringin, capecitabine, and their combination also increased the proportion of necrotic cells compared with the untreated control. However, no statistically significant difference in necrosis was observed among the treatment groups.

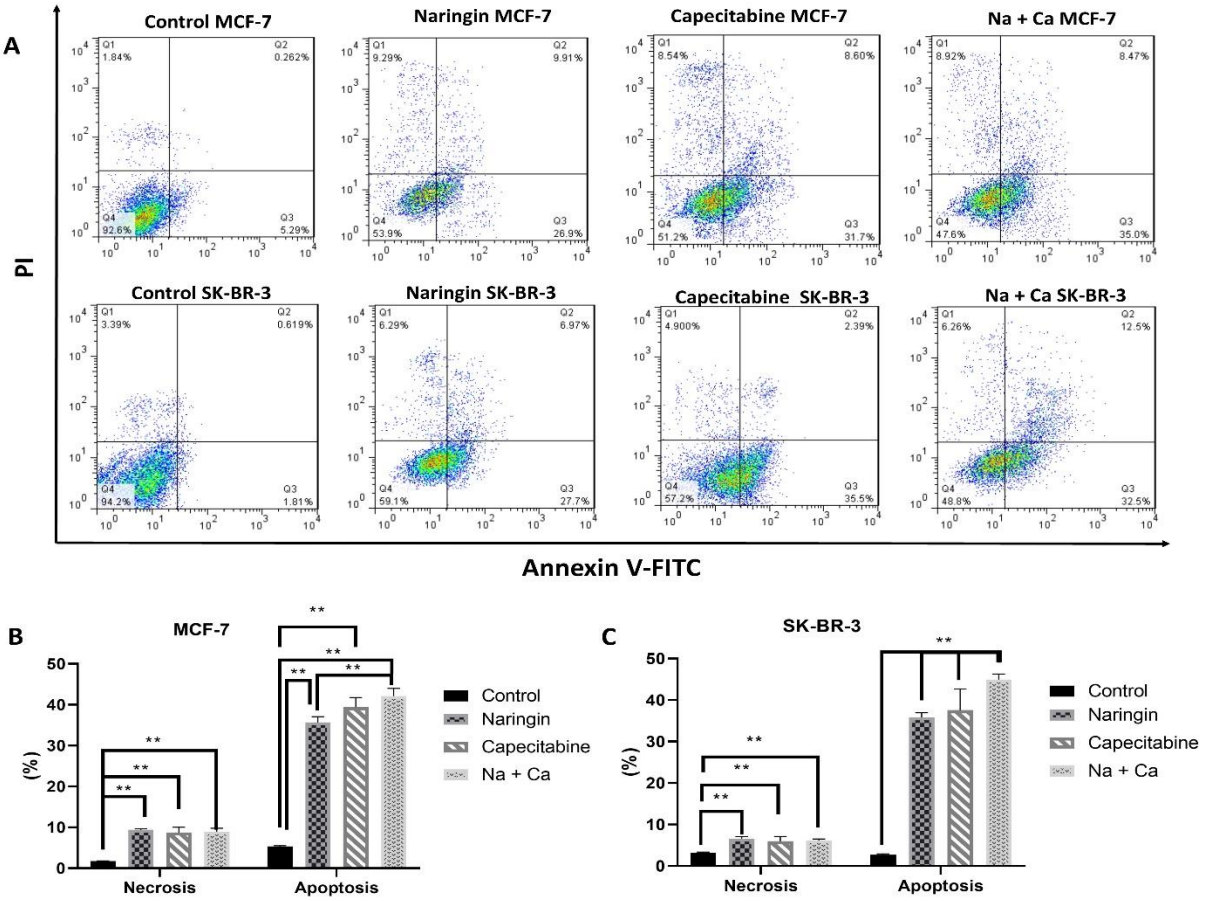

Figure 2: Effects of naringin and capecitabine on apoptosis and necrosis in MCF-7 and SK-BR-3 cells

Apoptosis and necrosis were assessed by Annexin V-FITC/PI flow cytometry. MCF-7 cells were treated for 24 h with naringin (58 µg/mL), capecitabine (619.36 µg/mL), or their combination (30.01 µg/mL naringin + 300.03 µg/mL capecitabine). SK-BR-3 cells were treated with naringin (56.65 µg/mL), capecitabine (679.51 µg/mL), or their combination (32.06 µg/mL naringin + 361.8 µg/mL capecitabine). Panel A shows representative Annexin V-FITC/PI plots; panels B and C show the percentages of apoptotic and necrotic MCF-7 and SK-BR-3 cells, respectively. Cells were classified as viable, early apoptotic, late apoptotic, or necrotic according to Annexin V/PI staining. Data are presented as mean ± SD of three independent biological experiments ($n = 3$). $P < 0.01$. Na, naringin; Ca, capecitabine.

We investigated the expression of genes involved in apoptosis after treatment with naringin and capecitabine on breast cancer cells (Figure 3). naringin-capecitabine increased *Bax* and *Caspase-3* gene expression and

decreased *Bcl-2* gene expression (Figures 3A and 3B). In the Sk-BR-3 cell line, the combined use of capecitabine and naringin also led to a significant increase in *Bax* and *Caspase-3* gene expression, as well as a significant decrease in *Bcl-2* gene expression compared with the use of these two substances alone ($P < 0.01$). In the MCF-7 cell line, naringin-capecitabine increased the expression of Bax and Caspase-3 genes and decreased the expression of Bcl-2, but these changes were not statistically significant compared with the use of capecitabine alone ($P > 0.05$). The Bax/Bcl-2 ratio is shown in Figure 3C. In MCF-7 cells, the Bax/Bcl-2 ratios were approximately 1.0 ± 0.1, 2.9 ± 0.2, 3.9 ± 1.1, and 6.9 ± 1.4 in the control, naringin, capecitabine, and naringin–capecitabine groups, respectively. In SK-BR-3 cells, the corresponding ratios were approximately 1.0 ± 0.1, 2.0 ± 0.2, 5.3 ± 0.2, and 10.1 ± 0.6, respectively. The combination treatment produced the highest Bax/Bcl-2 ratio in both cell lines ($P < 0.01$; $n = 3$).

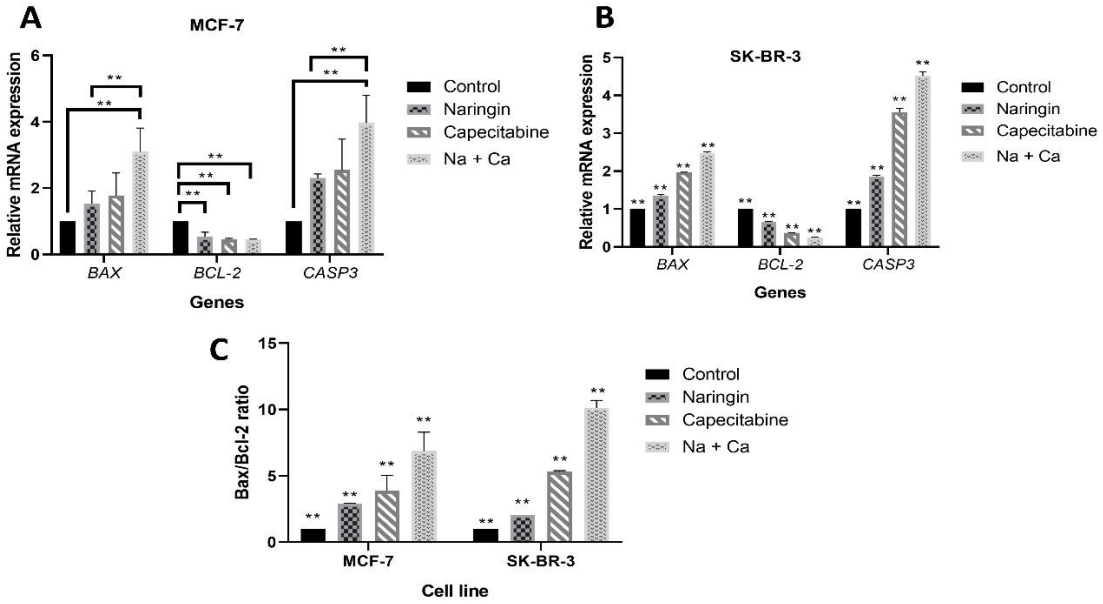

Figure 3: Relative expression of Bax, Bcl-2, and Caspase-3 in MCF-7 (A) and SK-BR-3 (B) cells and the Bax/Bcl-2 expression ratio (C). Data are presented as mean ± SD of three independent biological experiments (n = 3). $P < 0.01$. Na, naringin; Ca, capecitabine

Lipid peroxidation was assessed by measuring malondialdehyde (MDA) levels in MCF-7 and SK-BR-3 cells following treatment with naringin, capecitabine, and their combination. As shown in Figure 4A, MDA levels were significantly increased in the treatment groups compared with the untreated control group. In MCF-7 cells, the naringin–capecitabine combination resulted in a significantly greater increase in MDA levels compared with either naringin or capecitabine alone ($P < 0.01$). In contrast, in SK-BR-3 cells, MDA levels following combination treatment were not significantly different from those observed with capecitabine alone. These findings indicate a differential response of the two cell lines to the combination treatment with respect to lipid peroxidation.

LDH release was measured in the culture supernatant of MCF-7 and SK-BR-3 cells following treatment with naringin, capecitabine, and their combination. As shown in Figure 4B, naringin treatment increased LDH release in both cell lines compared with the untreated control group. Similarly, the naringin–capecitabine combination increased LDH levels compared with the control group. In contrast, capecitabine treatment alone did not significantly increase LDH release compared with the control group. The observed changes in LDH levels indicate alterations in cellular membrane integrity following treatment.

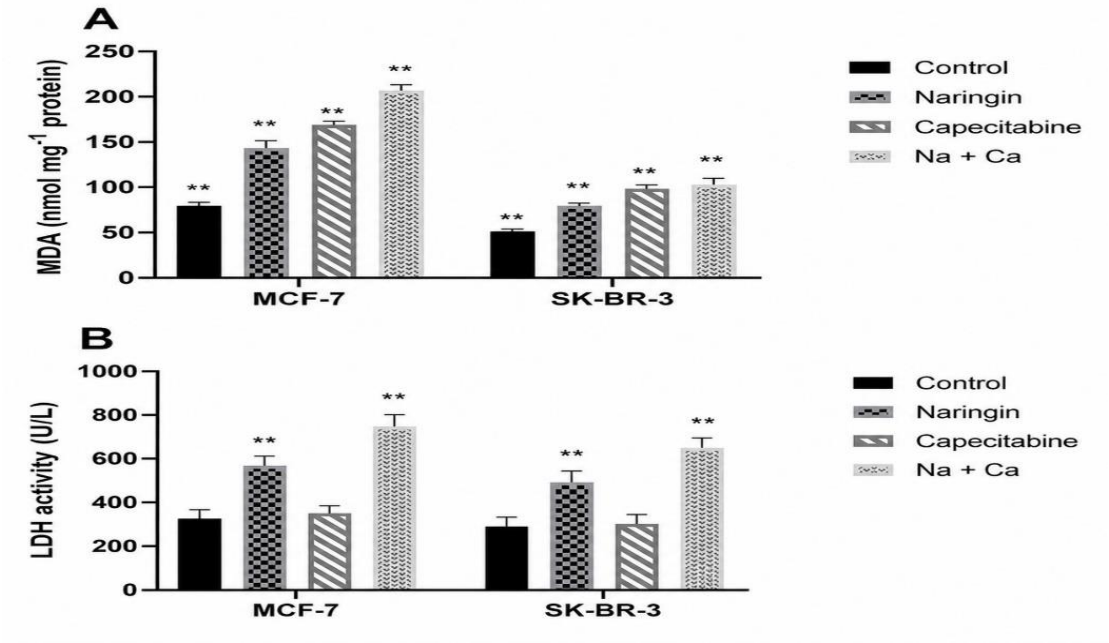

Figure 4: Effects of naringin, capecitabine, and their combination on malondialdehyde (MDA) levels (A) and lactate dehydrogenase (LDH) release (B) in MCF-7 and SK-BR-3 cells

Discussion

The present study investigated the cytotoxic and pro-apoptotic effects of naringin, capecitabine, and their combination in MCF-7 and SK-BR-3 breast cancer cells. Overall, combined treatment was associated with enhanced cytotoxicity, increased apoptosis, greater membrane damage, and increased lipid peroxidation compared with the individual treatments. However, the magnitude of these effects differed between the two cell lines, suggesting that cellular context may influence the response to naringin–capecitabine treatment [17-19].

Naringin is a citrus-derived flavonoid with several biological activities, including antioxidant and anticancer effects. Flavonoids are important plant-derived polyphenolic compounds that have been extensively investigated for their potential anticancer properties [21]. Previous studies have reported antiproliferative and pro-apoptotic effects of naringin in several cancer models. Park et al. demonstrated that naringin inhibited proliferation of THP-1 leukemia cells through induction of apoptosis [17], while Jarrett et al. reported cytotoxic effects of naringin in ovarian cancer cells [18]. More recently, the cytotoxic activity of naringin against MCF-7 breast cancer cells was also reported [19]. The present findings extend these observations by showing that naringin can enhance the cytotoxic response to capecitabine in MCF-7 and SK-BR-3 cells.

The reduction in the apparent IC50 of capecitabine in the presence of naringin suggests that naringin may increase cellular sensitivity to capecitabine. However, the individual-drug IC50 values were extrapolated from fitted dose–response curves rather than bracketed directly by the reported concentration range; therefore, these estimates require confirmation using broader concentration ranges that encompass the 50% response level. This finding provides a rationale for investigating naringin as a potential chemosensitising agent. However, a reduction in IC50 alone is insufficient to establish pharmacological synergy. Definitive demonstration of synergy requires multiple drug concentrations and ratios together with an appropriate quantitative combination-analysis method. Therefore, the present results should be interpreted as evidence of an enhanced interaction between naringin and capecitabine, while formal confirmation of synergy requires further dose–response and combination-index analyses.

The apoptotic findings provide a potential mechanistic explanation for the enhanced cytotoxicity. The intrinsic apoptotic pathway is closely regulated by the Bcl-2 protein family, and an increased Bax/Bcl-2 ratio is generally associated with mitochondrial apoptotic signalling and subsequent activation of the caspase cascade [22,23]. In the present study, naringin treatment was associated with downregulation of Bcl-2 and upregulation of Bax and Caspase-3, resulting in an increased Bax/Bcl-2 ratio. These

findings are consistent with previous reports indicating that modulation of the Bax/Bcl-2 axis contributes to the antiproliferative and pro-apoptotic effects of naringin [20]. Importantly, the combination treatment produced greater changes in apoptotic markers than capecitabine alone, suggesting that naringin may potentiate capecitabine-associated apoptotic signalling.

Caspase-3 is a key executioner caspase involved in the cleavage of cellular substrates during apoptosis and contributes to the characteristic morphological and biochemical changes associated with programmed cell death [24]. The increased *Caspase-3* expression observed in the present study, together with the flow-cytometric evidence of increased apoptosis, supports the involvement of apoptotic cell death in the response to naringin–capecitabine treatment. Nevertheless, gene-expression changes alone do not establish activation of the corresponding proteins. Therefore, confirmation at the protein level, particularly assessment of cleaved caspase-3, Bax and Bcl-2, would provide stronger mechanistic evidence.

An important finding was the differential response of MCF-7 and SK-BR-3 cells. The combination treatment produced significantly greater changes in the *Bax/Bcl-2* ratio and *Caspase-3* expression in SK-BR-3 cells than in MCF-7 cells. This difference may reflect the distinct molecular characteristics of these breast cancer cell lines. Because SK-BR-3 cells exhibit HER2 overexpression, whereas MCF-7 cells have a different receptor profile, differences in intracellular signalling, apoptotic susceptibility and drug responsiveness may contribute to the observed responses. However, the present study did not directly investigate HER2 signalling. Thus, the greater apoptotic response in SK-BR-3 cells should not be interpreted as proof that HER2 mediates the effect of the combination. Further studies incorporating HER2 expression/activity and pathway-specific inhibition or rescue experiments are required to test this hypothesis.

The LDH findings were consistent with treatment-associated disruption of cellular membrane integrity. LDH release increased following naringin and combination treatment compared with untreated cells, indicating increased cellular injury. However, LDH release is not specific for necrotic cell death and may occur following different forms of cellular damage. Therefore, the present LDH findings should be interpreted as evidence of membrane damage rather than definitive evidence of necrosis. The flow-cytometry results similarly demonstrated changes in membrane-compromised cells, but integration with additional cell-death markers would be required for more precise discrimination between apoptotic and necrotic processes. Previous work has also demonstrated that naringin can promote apoptosis without necessarily producing a corresponding increase in necrosis [25].

The observed increase in MDA provides evidence of altered lipid peroxidation following treatment. Notably, the combination produced a significantly greater increase in MDA than either treatment alone in MCF-7 cells, whereas no significant difference was observed between the combination and capecitabine alone in SK-BR-3 cells. This cell-line-dependent pattern suggests that lipid peroxidation may contribute differently to the response to combined treatment. Lipid peroxidation is an important feature of several forms of regulated cell death and is particularly relevant to ferroptosis [26]. Nevertheless, increased MDA alone cannot establish oxidative stress as the causal mechanism of cytotoxicity and is insufficient to demonstrate ferroptosis. Confirmation would require assessment of established ferroptosis-related pathways and markers, together with pharmacological inhibition or rescue experiments.

Taken together, the present findings suggest that naringin may enhance the anticancer activity of capecitabine in breast cancer cells, with increased apoptotic signalling and lipid peroxidation potentially contributing to the observed cytotoxic response. The stronger apoptotic response in SK-BR-3 cells further indicates that cellular molecular characteristics may influence the efficacy of the combination. However, the findings remain limited to an in-vitro model, and the precise molecular basis of the interaction requires further investigation. Future studies should confirm the observed changes at the protein level, determine the contribution of relevant signalling pathways, formally evaluate pharmacological synergy using appropriate combination designs, and investigate whether oxidative stress or ferroptosis contributes causally to cell death. In-vivo studies will ultimately be required to determine the therapeutic relevance and safety of the naringin–capecitabine combination.

Conclusion

MTT results showed good differentiation in cellular inhibition between capecitabine alone and narangin-capcitabine combination. The CI values indicated enhanced inhibitory interactions between naringin and capecitabine at most of the tested combinations, although an antagonistic interaction was observed at the lowest combination dose in

SK-BR-3 cells. The results indicate that naringin-capecitabine has a good apoptotic potential. Caspase-3, was more expressed by naringin+capecitabine. Overall, the results suggest that naringin–capecitabine-induced cell death may involve Caspase-3- and Bax/Bcl-2-associated apoptotic mechanisms. The magnitude of the antiproliferative response to the naringin–capecitabine combination differed between MCF-7 and SK-BR-3 cells, with greater activity observed in SK-BR-3 cells under the conditions tested. However, because these two cell lines differ in multiple molecular characteristics, the observed difference cannot be attributed specifically to HER2 status on the basis of the present study. Further studies incorporating direct assessment or modulation of HER2 signalling are required to determine whether HER2 contributes to the differential response.

Statements and Declarations

Funding support

The authors did not receive support from any organization for the submitted work.

Competing interests

The authors have no competing interests to declare that are relevant to the content of this article.

Ethics approval

This study was performed in line with the principles of the Declaration of Helsinki.

Consent to participate

Informed consent was obtained from all individual participants included in the study.

Authors' Contributions

The authors confirm contribution to the paper as follows: Study conception and design: Sanli Soltannezhad, Laya Takbiri Osgoei
Data collection: Sanli Soltannezhad, Laya Takbiri Osgoei, Analysis and interpretation of results: Sanli Soltannezhad, Fatemeh Javani Jouni, Draft manuscript: Laya Takbiri Osgoei, Sanli Soltannezhad Fatemeh Javani Jouni. All authors reviewed the results and approved the final version of the manuscript.

References

1. Siegel RL, Kratzer TB, Wagle NS, Sung H, Jemal A. Cancer statistics, 2026. CA Cancer J Clin. 2026;76(1):e70043. doi:10.3322/caac.70043.
2. Ardalan N, Akhavan Sepahi A, Khavari-Nejad RA. Development of Escherichia coli asparaginase II for the treatment of acute lymphocytic leukemia: in silico reduction of asparaginase II side effects by a novel mutant (V27F). Asian Pac J Cancer Prev. 2021;22(4):1137-47. doi:10.31557/APJCP.2021.22.4.1137.
3. Ardalan N, Mirzaie S, Sepahi AA, Khavari-Nejad RA. Novel mutant of Escherichia coli asparaginase II to reduction of the glutaminase activity in treatment of acute lymphocytic leukemia by molecular dynamics simulations and QM-MM studies. Med Hypotheses. 2018;112:7-17.
4. Momenimovahed Z, Salehiniya H. Epidemiological characteristics of and risk factors for breast cancer in the world. Breast Cancer (Dove Med Press). 2019;11:151-64. doi:10.2147/BCTT.S176070.
5. Adhami M, MotieGhader H, Haghdoost AA, Afshar RM, Sadeghi B. Gene co-expression network approach for predicting prognostic microRNA biomarkers in different subtypes of breast cancer. Genomics. 2020;112(1):135-43. doi:10.1016/j.ygeno.2019.01.010.
6. Sun GY, Jing H, Wang SL, Song YW, Jin J, Fang H, et al. Trastuzumab provides a comparable prognosis in patients with HER2-positive breast cancer to those with HER2-negative breast cancer: post hoc analyses of a randomized controlled trial of post-mastectomy hypofractionated radiotherapy. Front Oncol. 2021;10:605750. doi:10.3389/fonc.2020.605750.
7. Kong X, Gao R, Wang Z, Wang X, Fang Y, Gao J, et al. Melatonin: a potential therapeutic option for breast cancer. Trends Endocrinol Metab. 2020.
8. Miura K, Kinouchi M, Ishida K, Fujibuchi W, Naitoh T, Ogawa H, et al. 5-FU metabolism in cancer and orally-administrable 5-FU drugs. Cancers (Basel). 2010;2(3):1717-30. doi:10.3390/cancers2031717.
9. Zaki HM. Review on 5-fluorouracil (5-FU) as anticancer medication. Damanhour J Vet Sci. 2025;13(3):1-5.
10. Lluch A, Barrios CH, Torrecillas L, Ruiz-Borrego M, Bines J, Segalla J, et al. Phase III trial of adjuvant capecitabine after standard neo-/adjuvant chemotherapy in patients with early triple-negative breast cancer (GEICAM/2003-11_CIBOMA/2004-01). J Clin Oncol. 2020;38(3):203.
11. Önder T, Cengiz M, Koçoğlu SS, Ateş Ö, Yazıcı O, İnanç M, et al. Prognostic value of HER2 2+ expression in patients with TNBC receiving adjuvant capecitabine. Clin Transl Oncol. 2025;27(7):3121-9.
12. Saura C, Oliveira M, Feng YH, Dai MS, Chen SW, Hurvitz SA, et al. Neratinib plus capecitabine versus lapatinib plus capecitabine in HER2-positive metastatic breast cancer previously treated with ≥2 HER2-directed regimens: phase III NALA trial. J Clin Oncol. 2020;38(27):3138.
13. Xu B, Yan M, Ma F, Hu XC, Feng JF, Ouyang Q, et al. Pyrotinib or lapatinib plus capecitabine for HER2+ metastatic breast cancer (PHOEBE): a randomized phase III trial. J Clin Oncol. 2020.
14. Askandar RH, Sharifi F, Shayan S, Mohammadi H, Rahimi A, Ardalan N, et al. Early blockage of Mycobacterium tuberculosis cell-wall synthesis via EchA6 inhibition to overcome resistance strain: insights from umbrella sampling simulations. Curr Bioact Compd. 2023;19(10):2-17.
15. Seyedi SH, Alhagh MS, Ahmadizad M, Ardalan N, Hosseininezhadian Koushki E, Farshadfar C, et al. Structural screening into the recognition of a potent

inhibitor against non-structural protein 16: a molecular simulation to inhibit SARS-CoV-2 infection. J Biomol Struct Dyn. 2022;40(24):14115-30. doi:10.1080/07391102.2021.2001374.
16. Erdogan S, Doganlar O, Doganlar ZB, Turkekul K. Naringin sensitizes human prostate cancer cells to paclitaxel therapy. Prostate Int. 2018;6(4):126-35.
17. Park JH, Jin CY, Lee BK, Kim GY, Choi YH, Jeong YK. Naringenin induces apoptosis through downregulation of Akt and caspase-3 activation in human leukemia THP-1 cells. Food Chem Toxicol. 2008;46(12):3684-90.
18. Jarrett NM, Gloria JCR, Abirami M, Shyam SJ, Radhakrishnan S, Deepa S, et al. Cytotoxic and apoptotic effect of citrus flavonoid naringin in treating PA-1 ovarian cancer cells. Res J Pharm Technol. 2020;13(9):4051-4.
19. Noman AM, Sultan MT, Raza H, Imran M, Hussain M, Mujtaba A, et al. An updated review of the anticancer mechanisms and therapeutic potential of naringenin. Food Sci Nutr. 2025;13(7):e70626.
20. Lu WL, Yu CTR, Lien HM, Sheu GT, Cherng SH. Cytotoxicity of naringenin induces Bax-mediated mitochondrial apoptosis in human lung adenocarcinoma A549 cells. Environ Toxicol. 2020;35(12):1386-94.
21. Nabavi SM, Šamec D, Tomczyk M, Milella L, Russo D, Habtemariam S, et al. Flavonoid biosynthetic pathways in plants: versatile targets for metabolic engineering. Biotechnol Adv. 2020;38:107316.
22. Ebadollahi S, Pouramir M, Zabihi E, Golpour M, Aghajanpour-Mir M. The effect of arbutin on the expression of tumor suppressor P53, BAX/BCL-2 ratio and oxidative stress induced by tert-butyl hydroperoxide in fibroblast and LNcap cell lines. Cell J. 2021;22(4):532.
23. Wolf P, Schoeniger A, Edlich F. Pro-apoptotic complexes of BAX and BAK on the outer mitochondrial membrane. Biochim Biophys Acta Mol Cell Res. 2022;1869(10):119317. doi:10.1016/j.bbamcr.2022.119317.
24. Feng X, Wang YW, He SJ, Huang Q. The paradigm-shifting roles of caspase-3 in cancer: from death towards resuscitation. Cancer Cell Int. 2026;26(1):93.
25. Jin CY, Park C, Hwang HJ, Kim GY, Choi BT, Kim WJ, et al. Naringenin up-regulates the expression of death receptor 5 and enhances TRAIL-induced apoptosis in human lung cancer A549 cells. Mol Nutr Food Res. 2011;55(2):300-9.
26. Bucarey JL, Casas M, Espinosa A. Mitochondrial iron handling and lipid peroxidation as drivers of ferroptosis. Int J Mol Sci. 2026;27(5):2232.